Tripletstate decay kinetics of hydrated chlorophyll complexes

A. J. Alfano, M. S. Showell, and F. K. Fong

Citation: The Journal of Chemical Physics **82**, 765 (1985); doi: 10.1063/1.448501
View online: http://dx.doi.org/10.1063/1.448501
View Table of Contents: http://scitation.aip.org/content/aip/journal/jcp/82/2?ver=pdfcov
Published by the AIP Publishing

Triplet-state decay kinetics of hydrated chlorophyll complexes

A. J. Alfano,[a] M. S. Showell,[b] and F. K. Fong
Department of Chemistry, Purdue University, West Lafayette, Indiana 47907

(Received 28 November 1983; accepted 7 August 1984)

The triplet-state lifetimes of Chl a·H_2O, (Chl a·H_2O)$_2$, and (Chl a·$2H_2O$)$_n$ aggregates were investigated by fluorometric techniques. A kinetic model is developed to account for the experimental observations. Evidence for the suitability of a four-level system is provided to include possible two-photon excitations involving an excited triplet state T_2. In contrast to the dramatic dependence of the singlet-state lifetime of hydrated Chl a on the aggregate size, the triplet-state lifetimes of monomeric, dimeric, and polymeric Chl a aggregates in nonpolar hydrocarbon solvents are all found to be about 1.0–1.1 ms at temperatures < 120 K. The experimental observations support a localized Chl a aggregate triplet-state interpretation for negligibly small triplet exciton interactions. Annihilation effects observed in (Chl a·$2H_2O$)$_n$ are shown to be accompanied by shortening of the triplet-state lifetime, consistent with a four-level kinetic model.

I. INTRODUCTION

Several years ago photogalvanic activity of *in vitro* chlorophyll a-water complexes on platinum was demonstrated in this laboratory.[1,2] A photogalvanic cell consisting of a chlorophyll a/Pt photocathode vs a platinum anode was used to produce H_2 and O_2 from water splitting with visible light as the driving force. The chlorophyll on the platinum surface exists as aggregates of hydrated chlorophyll.[1,3] The photoactivity of a given Chl a-H_2O aggregate toward water splitting is expected to result from a combination of photophysical and redox properties.[1,4] In particular, the question of the involvement of triplet state and/or singlet–triplet annihilation effects in the photocatalytic activity of the chlorophyll is of interest.[1] In the preceding paper we reported[5] the singlet-state lifetimes of hydrated chlorophyll Chl a·H_2O and its dimeric and polymeric aggregates (Chl a·H_2O)$_2$ and (Chl a·$2H_2O$)$_n$ in homogeneous solutions. In this paper corresponding triplet-state lifetime measurements of these species are described.

The study of the triplet-state lifetimes of Chl a systems is complicated by their low (10^{-5}) phosphorescence quantum yield.[6] Optically detected magnetic resonance (ODMR),[7] transient absorption,[8–10] delayed fluorescence,[11] and even direct phosphorescence[12–15] techniques have been employed to obtain information on the triplet state of various chlorophyll aggregates and derivatives *in vitro*. Fluorometric techniques are employed in the present study to provide measurements of the triplet-state lifetimes τ_T of Chl a·H_2O, (Chl a·H_2O)$_2$, (Chl a·$2H_2O$)$_n$, and pheophytin a. Our results compare with τ_T values previously reported for monomeric Chl a, and provide additional information on hitherto unreported triplet decay kinetics of aggregated Chl a complexes.

In the limit of zero source intensity the maximum T_1 lifetime τ_T^0 given by the reciprocal of the $T_1 \rightarrow S_0$ transition rate constant, is obtained. Under practical conditions the apparent triplet lifetime τ_T may be shortened by the excitation of T_1 to a higher triplet state T_2 provided that the crossing over to the singlet manifold from T_2 is sufficiently rapid (i.e., the k_5 process in Fig. 3). The experiments in this work ascertain the triplet lifetimes of Chl a samples in which the probability of $T_1 \rightarrow T_2$ transition is minimized. Triplet-state lifetime shortening as a result of singlet–triplet annihilation is then demonstrated on comparison with the results thus obtained. The experimental observations are accounted for using a four-level kinetic model consisting of the two lowest-lying states S_0 and S_1 from the singlet manifold and the other two T_1 and T_2 from the triplet manifold. An important conclusion is that T_1 is not delocalized by exciton interactions upon Chl a aggregation.

II. KINETIC MODEL

The photophysical states of the chlorophyll molecule, like those of other macrocyclic systems, are grouped into singlet and triplet manifolds. Internal conversions within the excited singlet and triplet manifolds are evidently so rapid that fluorescence is observed only from the first excited singlet state[16] S_1 and phosphorescence is expected only from the lowest triplet state T_1.[17] Even so, the measurement of the T_1 lifetime is made difficult by the fact that direct phosphorescence is not easily observed in Chl a systems.[6] Accordingly it seems desirable to derive triplet lifetimes from photophysical properties of the fluorescent S_1 state, which is kinetically coupled to the T_1 state. This section provides the mathematical framework for describing the fluorescent response of a multilevel photophysical system to modulated light when the modulation period is several times longer than the triplet state lifetime ($\sim 50\%$ duty cycle).

A first attempt towards a rigorous analysis is the three-level system (Fig. 1) in which we have

$$[S_0] + [S_1] + [T_1] = C, \tag{1}$$

where C is the sample molarity and $[i]$ is the molarity of state i. The kinetic relationships are given by:

$$d[S_0]/dt = k_1[S_1] - k_0[S_0] + k_3[T_1], \tag{2}$$

$$d[S_1]/dt = k_0[S_0] - (k_1 + k_2)[S_1], \tag{3}$$

$$d[T_1]/dt = k_2[S_1] - k_3[T_1], \tag{4}$$

where k_1, k_2, and k_3 are, respectively, the rate constants attending the $S_1 \rightarrow S_0$, $S_1 \rightarrow T_1$, and $T_1 \rightarrow S_0$ transitions. The constant k_0 is a product of the source intensity, the wave-

[a] Present address: Rockwell Science Center, Thousand Oaks, CA 91360.
[b] Present address: Ivorydale Technical Center, Procter and Gamble Co., Cincinnati, OH 45217.

 0021-9606/85/020765-08$02.10

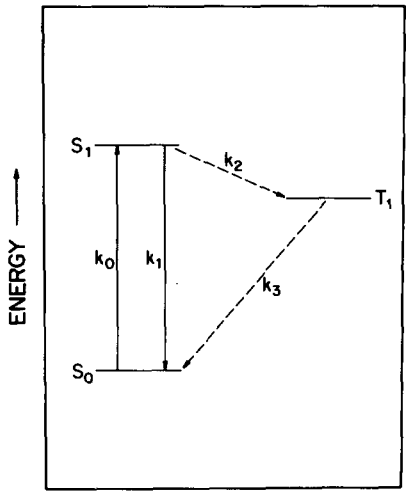

FIG. 1. Three-level photophysical scheme. The rate constants k_1, k_2, and k_3, respectively, correspond to the transitions $S_1 \rightarrow S_0$, $S_1 \rightarrow T_1$, and $T_1 \rightarrow S_0$. The rate constant k_0 attending the $S_0 \rightarrow S_1$ transition is dependent on the source intensity and the absorption coefficient of the chlorophyll.

length dependent absorption coefficient, and a loss coefficient for the optical system. Equation (1) is solved for $[S_1]$ and substituted into Eq. (4), which yields upon differentiation

$$\frac{d^2[T_1]}{dt^2} = -(k_2+k_3)\frac{d[T_1]}{dt} - k_2\frac{d[S_0]}{dt}. \tag{5}$$

The value of $d[S_0]/dt$ is substituted from Eq. (2) and $[S_0]$ replaced upon rearrangement of Eq. (1) to give the second-order linear differential equation

$$\frac{d^2[T_1]}{dt^2} + (\alpha+\beta)\frac{d[T_1]}{dt} + \alpha\beta[T_1] = k_0k_2C, \tag{6}$$

where the constant coefficients α and β are given by

$$\alpha+\beta = k_0+k_1+k_2+k_3 \tag{7}$$

and

$$\alpha\beta = k_1k_3 + k_2k_3 + k_0k_2 + k_0k_3. \tag{8}$$

The corresponding complementary and particular solutions to Eq. (6) are added to give the general solution

$$[T_1] = C_1\exp(-\alpha t) + C_2\exp(-\beta t) + (k_0k_2C/\alpha\beta). \tag{9}$$

On combining Eqs. (1), (4), and (9) we write

$$[S_0] = C + \frac{(\alpha-k_2-k_3)}{k_2}C_1\exp(-\alpha t) + \frac{(\beta-k_2-k_3)}{k_2}C_2\exp(-\beta t) - \frac{(k_2+k_3)k_0C}{\alpha\beta}. \tag{10}$$

This time dependence of $[S_1]$ is found from Eqs. (4) and (9):

$$[S_1] = \frac{(k_3-\alpha)}{k_2}C_1\exp(-\alpha t) + \frac{(k_3-\beta)}{k_2}C_2\exp(-\beta t) + \frac{k_0k_3C}{\alpha\beta}. \tag{11}$$

The specification of the constants C_1 and C_2 in Eqs. (9)–(11) requires the imposition of initial conditions applicable to the situations to be described below. The experimental arrangements are designed to monitor the S_1 fluorescence under two different modulation conditions in order to obtain the two different sets of conditions at time zero:

$$[S_1] = [T_1] = 0, \quad [S_0] = C \tag{12}$$

and

$$[S_1] = 0, \quad [T_1] = xC, \quad [S_0] = (1-x)C. \tag{13}$$

Physically, the two situations correspond to the onset of excitation in a system where appreciable triplet state concentration remains from the previous modulation cycle [Eq. (13)] and where both singlet and triplet manifolds have relaxed [Eq. (12)]. The quantity x represents the fraction of Chl a stored in the triplet state at the beginning of excitation. Simultaneous solutions of Eqs. (9)–(11) under conditions (12) and (13), respectively, yields

$$C_1 = \frac{Ck_0k_2}{\alpha(\alpha-\beta)}; \quad C_2 = \frac{Ck_0k_2}{\beta(\beta-\alpha)} \tag{14}$$

and

$$C_1 = \frac{Ck_0k_2}{\alpha(\alpha-\beta)} - \frac{xC(k_3-\beta)}{(\beta-\alpha)};$$
$$C_2 = \frac{Ck_0k_2}{\beta(\beta-\alpha)} - \frac{xC(\alpha-k_3)}{(\beta-\alpha)}. \tag{15}$$

With fluorescence as a probe, only the expressions for $[S_1]$ as a function of time are of practical importance. Substitution of Eqs. (14) and (15) into Eq. (11) yields, respectively,

$$[S_1] = Ck_0\left[\frac{k_3}{\alpha\beta} + \frac{(k_3-\alpha)}{\alpha(\alpha-\beta)}\exp(-\alpha t) + \frac{(k_3-\beta)}{\beta(\beta-\alpha)}\exp(-\beta t)\right] \tag{16}$$

and

$$[S_1] = \frac{Ck_0k_3}{\alpha\beta} + \left[\frac{(k_3-\alpha)Ck_0}{\alpha(\alpha-\beta)} - \frac{(k_3-\alpha)xC(k_3-\beta)}{k_2(\beta-\alpha)}\right]\exp(-\alpha t) + \left[\frac{(k_3-\beta)k_0A}{\beta(\beta-\alpha)} - \frac{(k_3-\beta)(\alpha-k_3)xC}{k_2(\beta-\alpha)}\right]\exp(-\beta t). \tag{17}$$

Solving Eqs. (7) and (8) for α and β we obtain

$$\alpha = \tfrac{1}{2}(k_0+k_1+k_2+k_3) + \tfrac{1}{2}[(k_0+k_1+k_2-k_3)^2 - 4k_0k_2]^{1/2}, \tag{18}$$

$$\beta = \tfrac{1}{2}(k_0+k_1+k_2+k_3) - \tfrac{1}{2}[(k_0+k_1+k_2-k_3)^2 - 4k_0k_2]^{1/2}. \tag{19}$$

Since the fluorescence lifetimes of chlorophyll species ($\sim$50 ps$\rightarrow$7 ns) are at least six orders of magnitude less than the triplet lifetimes ($\sim$1 ms)[5] and the triplet quantum yield is appreciable,[8] it follows that $k_1 \simeq k_2 \gg k_0 \simeq k_3$, ($k_0 \simeq 10^3$ s^{-1} typically). These inequalities give $\alpha \gg \beta$ and $\exp(-\alpha t) \ll \exp(-\beta t)$, so Eqs. (16) and (17) may be simplified to read, respectively,

$$[S_1] = (Ck_0k_3/\alpha\beta)[1 + (\beta/k_3 - 1)\exp(-\beta t)], \tag{20}$$

$$[S_1] = \frac{Ck_0k_3}{\alpha\beta}\left[1 - (\beta/k_3 - 1)\left(\frac{\alpha\beta x}{k_0k_2} - 1\right)\exp(-\beta t)\right]. \quad (21)$$

Both of the above expressions indicate that square-wave modulation of the exciting light gives rise to a nonsquare-wave fluorescent response as shown in Fig. 2. Figure 2(b) corresponds to Eq. (20) and demonstrates that the fluorescence exponentially decays to a steady-state level. Figure 2(c) corresponds to Eq. (21) and indicates that the fluorescence rises to a steady-state level. In either case the exponential dependence involves β from Eq. (19) which becomes k_3, the reciprocal of the triplet lifetime, τ_T^0, in the limit of low light intensity (i.e., $k_0 \to 0$). The result in Eq. (20) is in agreement with that of Nakamizo and Matsueda[17] who considered only the initial conditions in Eq. (12).

A more realistic situation includes a higher triplet state to give the four-level system in Fig. 3. Specification of the kinetic relationships for this case requires the solution of a third-order linear differential equation analogous to Eq. (6). The resulting equations for the time dependence of each state are sums of three exponential terms involving the decay constants for S_1, T_1, and T_2. With the reasonable assumption of rapid decay kinetics for higher states within a given manifold, simplified expressions involving a single exponential containing the lowest triplet state T_1 lifetimes at low flux are again obtained. In this case, the inclusion of any conceivable two-photon process capable of populating higher triplet states (e.g., $T_1 \to T_2$ absorption or S_1–T_1 annihilation) reduces to the same result. An expression of the form of Eq. (16) is obtained[18] with

$$\alpha = k_1 + k_2, \quad (22)$$

$$\beta = k_3 + k_0\left(\frac{k_2}{k_1 + k_2}\right) + \frac{k_4}{R}\left(k_7 + \frac{k_1k_5}{k_1 + k_2}\right), \quad (23)$$

$$R = k_5 + k_6 + k_7, \quad (24)$$

where k_5, k_6, and k_7 denote the rate constant for the $T_2 \to S_1$, $T_2 \to T_1$, and $T_2 \to S_0$ transitions, and k_4 refers to triplet–triplet excitation and is source intensity dependent. In Eqs. (22) and (23), α and β are the rate constants for S_1 and T_1 decay, so the singlet and triplet lifetimes τ_S and τ_T are, respectively, given by α^{-1} and β^{-1}. In Eq. (23) the third term is the contribution to T_1 decay from the second-stage excitation of the triplet to T_2. In the limit of low k_0 and k_4, which are both proportional to I_0, the incident light flux, the expressions for α and β in Eqs. (22) and (23) asymptotically approach those given in Eqs. (18) and (19), respectively.

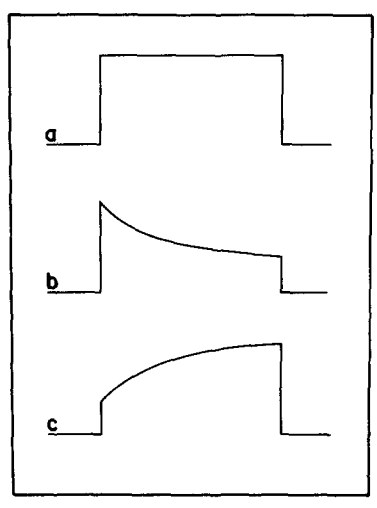

FIG. 2. Model response of S_1 fluorescence to modulated light. (a) Square wave modulation of the excitation source; (b) fluorescent decay to a steady-state level during single-beam excitation according to Eq. (20); (c) fluorescent rise to a steady-state level in double-beam excitation experiment as predicted by Eq. (21).

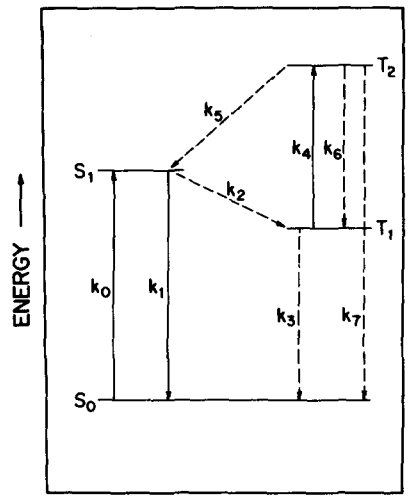

FIG. 3. Four-level model scheme. The rate constant k_0, k_1, k_2 and k_3 are the same as those in Fig. 1; the rate constant k_4 attending the $T_1 \to T_2$ transition is dependent on the source intensity; the rate constants k_5, k_6, and k_7, respectively, correspond to the transitions $T_2 \to S_1$, $T_2 \to T_1$, and $T_2 \to S_0$.

The mathematical relationships derived above are used to interpret the results of experiments described herein. In one type of experiment a single mechanically modulated (< 100 Hz) argon ion laser is used to excite the Chl *a* fluorescence. Although the modulation is square wave (> 5 ms light, > 5 ms dark), the fluorescence rises instantaneously and exponentially decays to a steady-state level in a few milliseconds after the onset of excitation in each modulation cycle. This exponential decay to a steady-state fluorescence reflects the accumulation of a triplet-state population. During the dark portion of each modulation cycle, the triplet population intersystem crosses back to the ground singlet state. At the onset of excitation the conditions $[S_1] = [T_1] = 0$ and $[S_0] = C$ prevail as in Eq. (12). The fluorescent temporal behavior during the light period is given by Eq. (20).

In the second type of experiment a low-power (2 mW) cw He–Ne laser is used in conjunction with the modulated argon ion laser to simultaneously excite the same sample region. Immediately after the argon ion laser is blocked, the He–Ne laser excites fluorescence in a sample with a significant triplet population. Therefore the fluorescence due to the He–Ne laser at the *cessation* of argon ion excitation displays an exponential growth to steady state. Although the He–Ne laser is not chopped, the fluorescence it induces at the beginning of the dark portion of the argon ion modulation cycle is described by Eq. (21) which results from the initial conditions in Eq. (13). The two experimental configurations described above are, respectively, referred to as single- and double-laser experiments in the next section.

III. EXPERIMENTAL

Chlorophyll *a* was extracted from fresh spinach according to well established column chromatographic proce-

dures.[1] The Chl *a* purity was established by absorption spectrophotometry using the criteria of band maxima position and blue-red peak absorbance ratios.[9,19] The Chl *a* extract was stored in *n*-pentane (water saturated) under argon atmosphere at 10 °C in the dark.

Sample A was prepared by diluting an aliquot of fresh stock Chl *a* solution with water-saturated methylcyclohexane (MCH) to give a 10^{-4} M solution in 1:1 MCH/n-pentane. Sample B containing 10^{-5} M Chl *a* was prepared according to the procedure of Hoshino *et al.*[20] to yield predominantly the (Chl *a*·H_2O)$_2$ aggregate[20,21] upon cooling to 77 K. Sample C was 10^{-5} M pheophytin *a* (Pheo *a*) in 1:1 MCH/*n*-pentane. The Pheo *a* was derived from stock Chl *a* by the procedure of Smith and Benitez.[22] Samples D and E containing 10^{-4} M Chl *a* in 1:1 MCH/*n*-pentane, in which (Chl *a*·$2H_2O$)$_n$ occurs in progressively larger concentrations, were prepared from stock solutions stored under an Ar atmosphere in the dark at 10 °C for six and eight weeks, respectively. The various samples were deoxygenated and sealed under vacuum ($< 10^{-4}$ Torr) in 4 mm o.d. Pyrex glass tubing.

The instrumentation utilized in the single- and double-laser, modulated fluorescence experiments has been described elsewhere.[23] The samples were positioned either in an Oxford Instruments DN704 variable temperature (300–77 K) cryostat or in an optical immersion Dewar (77 K). The Dewar was used to quench cool samples to 77 K. A Digital Equipment Corporation PDP-8/L computer, triggered by a mechanical light chopper (< 100 Hz), was utilized for data acquisition and storage. Sampling and digitization was delayed with software to start at the desired point on the modulation square wave. Sampling at either 184 or 31 μs per point was used throughout. Typically 500–1000 repetitions were stored, averaged, and output to a teletype. Fluorescence spectra were obtained according to the procedure of Alfano and Fong.[23]

IV. RESULTS

A. Fluorescence spectra

The 77 K fluorescence spectrum of sample A, cooled from room temperature at 2 deg/min, is reproduced in Fig. 4. The 684 nm peak is attributed to monomeric chlorophyll *a*, Chl *a*·H_2O, and the weaker band at 747 nm is attributed to the polymeric aggregate (Chl *a*·$2H_2O$)$_n$.[4,21] Quench cooling of sample B to 77 K results predominantly in the formation of (Chl *a*·H_2O)$_2$ which has a fluorescence maximum at 720 nm[20,21] (Fig. 5). Sample C containing Pheo *a* displays a fluorescence spectrum with a peak maximum at 705 nm (Fig. 6) after quench cooling to 77 K.

B. Modulation of fluorescence

The Dewar, detection and signal processing components and only a modulated argon ion laser (90 Hz) were used in the single-laser excitation experiments.[23] Using sample A (slowly cooled to 77 K) and the monochromator set at 684 and 747 nm, the fluorescent response during the light portion of the modulation cycle is shown in Figs. 7(a) and 7(b), respectively. The results thus obtained are in qualitative agreement with Eq. (20) for both Chl *a*·H_2O and (Chl *a*·$2H_2O$)$_n$. The sampling rate was 31 μs/point and 1000 repetitions were averaged. The density of data points collected is roughly three times that shown in Fig. 7.

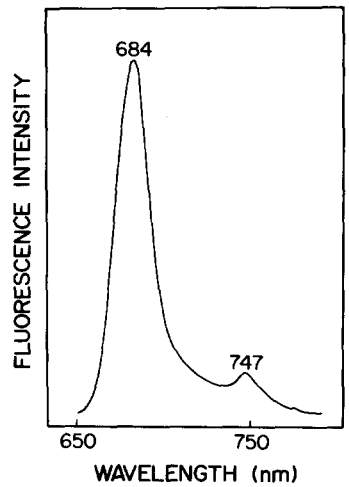

FIG. 4. The 77 K fluorescence spectrum of 10^{-4} M Chl *a* in water-saturated 1:1 *n*-pentane and methylcyclohexane.

Figure 8 is a plot of β, (BETA) obtained from least squares fits of Eq. (20) to results similar to those in Fig. 7 at several intensities for both Chl *a*·H_2O and (Chl *a*·$2H_2O$)$_n$. According to Eq. (23) the data points are least squares fits to a linear functional form in the light intensity I (k_0 and k_4 are proportional to I) yielding a zero-light limit value for the triplet lifetime $\tau_T^0 = k_3^{-1}$ of 0.8 ms for both Chl *a*·H_2O and (Chl *a*·$2H_2O$)$_n$.

In a typical double-laser excitation experiment, a cw He–Ne and a modulated argon ion laser are used to irradiate the same sample region.[23] Data collection is begun just prior to the beginning of the dark portion of the argon ion laser modulation cycle and the fluorescence due to the He–Ne laser follows Eq. (21). Typical results are shown in Fig. 9. The relative diminution in fluorescence intensity at time zero is related to the argon ion laser intensity but β in Eq. (21) is determined by the unfocused, low power (2 mW) He–Ne

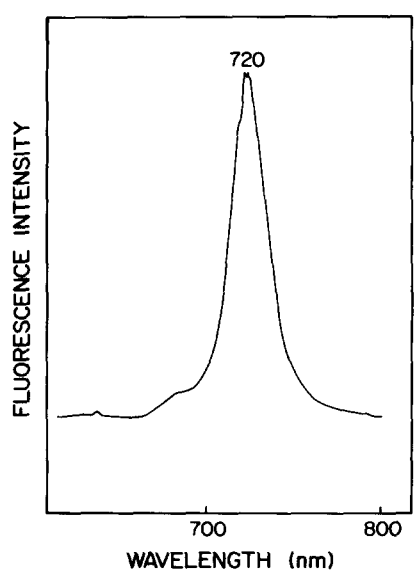

FIG. 5. The 77 K fluorescence spectrum of (Chl *a*·H_2O)$_2$ obtained from a 10^{-5} M Chl *a* solution in 3-methylpentane solvent.

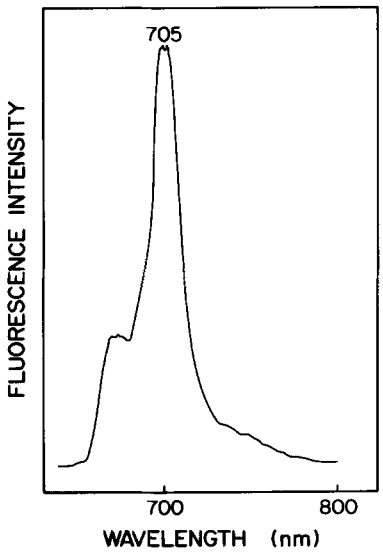

FIG. 6. Fluorescence spectrum, at 77 K, of 10^{-5} M Pheo *a* in water-saturated 1:1 *n*-pentane and methylcyclohexane.

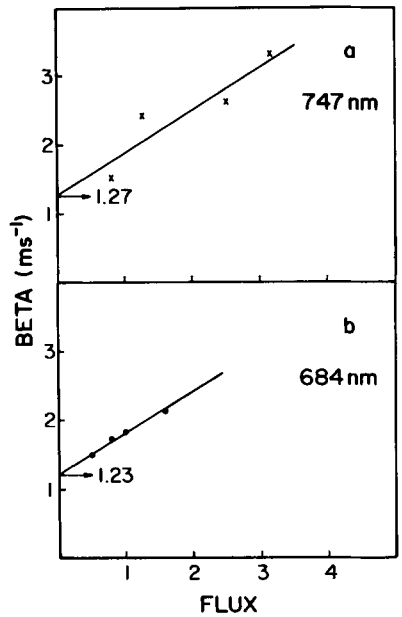

FIG. 8. Intensity dependence of β (BETA) for the sample in Fig. 4. Fluorescence decay curves of the type shown in Fig. 7, measured at several values of the Ar^+-laser excitation intensity, were least squares fitted to Eq. (20) to obtain β. (a) Detection at the 747 nm (Chl a·$2H_2O)_n$ fluorescence band; (b) detection at the 684 nm fluorescence band of monomeric Chl *a*. The data points in (a) and (b) are least-squares fitted (solid lines) to a linear dependence in I, the incident source intensity. The intercepts give a zero-light-limit value for the triplet lifetime $\tau_T^0 = \beta^{-1}(I \to 0)$, of 0.8 ms for both Chl a·H_2O and (Chl a·$2H_2O)_n$.

laser. Figures 9(b) and 9(d) correspond to sample A (77 K) with ~20 mW of focused argon radiation and with fluorescence detection at 747 and 684 nm, respectively. Least squares fits to the data acquired at 31 μs/point give a value for β^{-1} of 1.0 ± 0.2 ms for both (Chl a·$2H_2O)_n$ and Chl a·H_2O. Values of $\beta^{-1} \equiv \tau_T$ were also measured with a sampling rate of 184 μs/point for Pheo *a* at 705 nm and (Chl a·$H_2O)_2$ at 720 nm for quench-cooled samples C and B, respectively. Typical results appear in Figs. 9(a) and 9(c). The triplet lifetimes thus obtained for Pheo *a* and (Chl a·$H_2O)_2$ are 0.6 ± 0.1 and 1.0 ± 0.1 ms, respectively.

The inset in Fig. 10 displays the 77 K fluorescence spectra, excited by 632.8 nm He–Ne laser radiation of samples A, D, and E. The growth of the unsymmetrical band in the 700–800 nm wavelength region of these spectra, attributable[4] to (Chl a·$2H_2O)_n$ fluorescence, reflects the increased Chl *a* aggregation on stock solution aging. The effect of increasing (Chl a·$2H_2O)_n$ concentration on the 77 K fluorescence quenching decay rate is shown in Fig. 10. The fluorescence signal at time t, FS(t), is normalized to that, FS(0), observed at $t = 0$ when the Ar^+ beam is cut off. Both FS(0) and FS(t) are measured relative to the steady-state fluorescence level established by the cw He–Ne beam. Figure 10(a) depicts the rate of fluorescence quenching decay, observed at 679 nm, of sample A. Quenching of the 733 nm fluorescence of sample D is shown in Fig. 10(b). The fluorescence quenching decay, observed at 744 nm, for sample E is shown in Fig. 10 (c). The slopes of the least squares fits (solid lines) to the data in Figs. 10(a)–10(c) directly yield the apparent triplet lifetimes τ_T of the corresponding Chl *a* species. The values 1.0 ± 0.2, 0.7 ± 0.2, and 0.6 ± 0.2 ms are obtained from the fits in Figs. 10(a), 10(b), and 10(c), respectively.

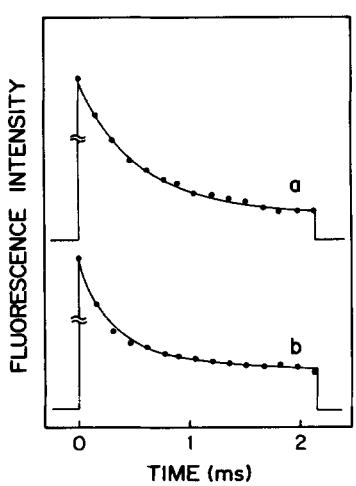

FIG. 7. Fluorescent decay, at 77 K, of the sample from Fig. 4 under single-beam excitation by a modulated Ar^+-laser source. (a) Monomer fluorescence decay monitored at 684 nm; (b) 747 nm fluorescence decay of (Chl a·$2H_2O)_n$.

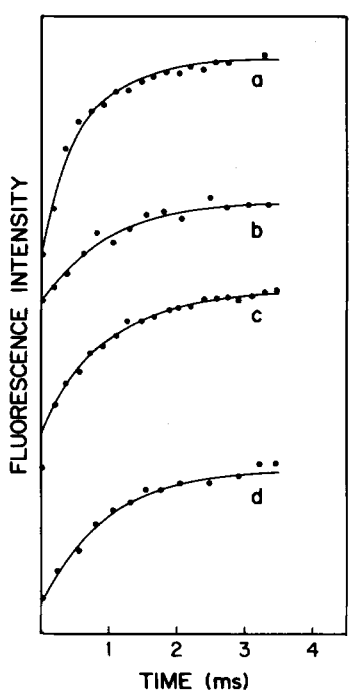

FIG. 9. Quenching of the 77 K fluorescence of (a) the sample in Fig. 6 at 705 nm; (b) the same as that in Fig. 4 at 747 nm; (c) the same as that in Fig. 5 at 720 nm; and (d) the same as that in Fig. 4 at 684 nm. The solid lines are least-squares fits to the data using Eq. (21).

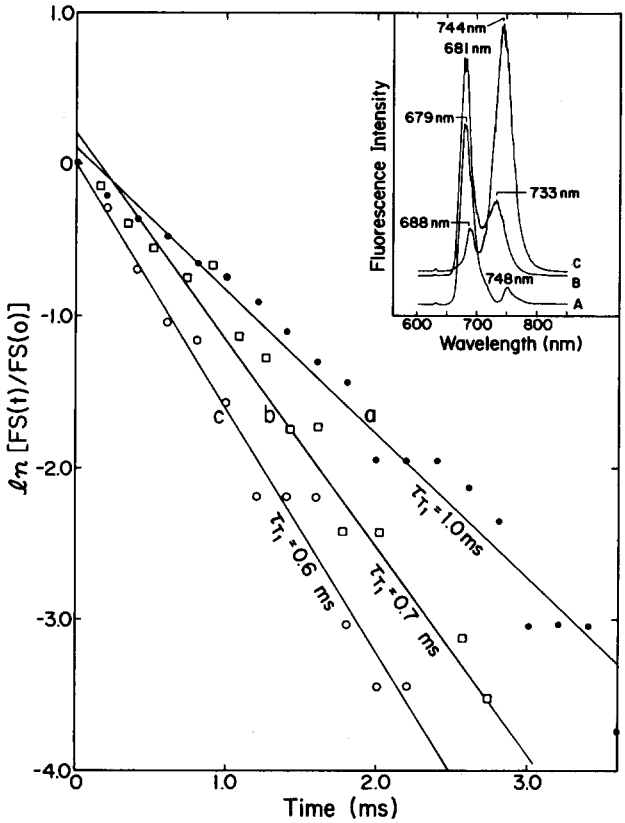

FIG. 10. Chl *a* fluorescence quenching decay at 77 K. FS (0) denotes the fluorescence signal, in mV, at $t = 0$ when the Ar^+ beam is cut off, and FS(t) is the fluorescence signal at time t. FS(0) and FS(t) are measured relative to the steady-state level established by the cw He–Ne beam. (a) 679 nm fluorescence quenching (●) of the sample shown in inset A; (b) quenching of the 733 nm fluorescence (□) corresponding to spectrum B in the inset; and (c) 744 nm fluorescence quenching (○) of the sample in inset C. The slopes of the least squares fits (solid lines) to the data in (a)–(c) directly yield the apparent triplet lifetimes τ_T of the corresponding Chl *a* species. The values 1.0, 0.7, and 0.6 ms are obtained from the fits in (a)–(c), respectively. Inset: 77 K fluorescence spectra of deoxygenated chlorophyll *a* solutions in 1:1 *n*-pentane/methylcyclohexane. Traces A–C were obtained from samples containing progressively larger amounts of (Chl *a*·$2H_2O$)$_n$. Recorder amplification is not constant. The dark storage times of the samples in B and C were six and eight weeks, respectively.

V. DISCUSSION

The results for the single laser experiments in Fig. 8 suggest that a four-level scheme including the T_2 state provides a reasonable account of the observations according to Eqs. (20) and (23). These single-laser experiments were also helpful in establishing the accuracy and desirability of the double-laser experiment which allows simpler data interpretation at the expense of somewhat more tedious optical alignment. A summary of representative triplet lifetimes obtained with the double-laser technique is given in Table I. Uncertainties are 95% confidence limits on the precision of the fit.

Parker and Joyce[11] employed a delayed fluorescence method to obtain a triplet lifetime of Chl *a* in ethanol of 0.87 ms at 21 °C, while Linschitz and Sarkanen[8] obtained 1.5 ms for Chl *a* in pyridine at 25 °C by transient absorption techniques. The chlorophyll in both of these studies was monomeric. Direct phosphorescence measurements[12] have been made on monomeric Chl *a*·H_2O yielding a triplet lifetime of 1.10 ± 0.05 ms at 77 K, in good agreement with our present value of 1.0 ± 0.2 ms. Evidently porphyrin triplet state lifetimes are very sensitive to the ligand coordination of the central metal atom,[12] deuteration of the metal-coordinating nucleophiles,[12,13] and substituent structure on the macrocycle periphery.[12,13] For example, in very dry ether where chlorophyll molecules are intermolecularly linked via carbonyl-Mg interactions the triplet lifetime is 5.1 ± 0.2 ms.[12] Ligation of the central magnesium atom with water lowers τ_T to 1.1 ± 0.05 ms.[12] The effect of deuteration is illustrated by the Chl *a*·EtOH series[12]: Chl *a*·C_2H_5OH (1.24 ± 0.05 ms); Chl *a*·C_2H_5OD (1.45 ± 0.05 ms); and Chl *a*·C_2D_5OD (1.60 ± 0.05 ms); all at 77 K. In ethanol at 77 K the triplet lifetime of Mg $\alpha, \beta, \gamma, \delta$ tetraphenylporphin is 37 ms,[13] Chl *b* is 3.0 ms, and Chl *a* is 1.24 ms.[12,14] The large difference in τ_T between Chl *a* and Chl *b* results from replacement of the methyl group on ring II of Chl *a* with HCO in Chl *b*.

TABLE I. Triplet state lifetimes at 77 K.

Species	Triplet Lifetime (ms)
Chl *a*·H_2O	1.0 ± 0.2
(Chl *a*·H_2O)$_2$	1.0 ± 0.1
(Chl *a*·$2H_2O$)$_n$	1.0 ± 0.2
Pheo *a*	0.6 ± 0.1

When the solvent system is nonpolar, the lack of a significant difference among the τ_T values for the three Chl *a* aggregates in Table I is clear. An optically detected magnetic resonance (ODMR) measurement of the monomer and dimer triplet decay rates arrived at a similar conclusion.[7] On the other hand upon changing the solvent polarity, Hoshino *et al.*[10] reported $\tau_T = 1.5$ and 2.0 ms for (Chl *a*·H_2O)$_2$ in 3-methylpentane and monomeric Chl *a* in 2-methyl tetrahydrofuran, respectively, at 77 K using transient absorption techniques.

It appears that apart from the effects of nucleophilic ligation to the Chl *a* Mg atom the intermolecular hydrogen bonding interactions leading to the aggregation of hydrated Chl *a* have little effect on the triplet-state kinetics of the chlorophyll. This is in contrast to the changes observed in the absorption and fluorescence spectra and the dependence of the singlet-state decay kinetics[5] on the Chl *a* aggregate size. In the latter case, the linear proportionality of the decay rate to the aggregate size n can be accounted for by an exciton description of the S_1 state.[5] The fact that τ_T does not observe a similar dependence on n (Table I) suggests that triplet exciton interactions in hydrated Chl *a* aggregates are small so that triplet excitation is effectively localized. This conclusion is apparently supported by recent studies of dimeric Chl *a* aggregates *in vitro*[10] and *in vivo*.[24]

Triplet excitons and excimers have been extensively studied in aromatic hydrocarbons.[25–28] The importance of an exiton-coupled triplet state in the C_2 symmetrical (bacterio) chlorophyll-*a* monohydrate dimer was previously considered.[29] It was noted that exciton interactions in the triplet manifold are small in comparison to those in the singlet manifold. In the formation of triplet excitons[30,31] electron exchange is usually a dominant factor in the case of aromatic hydrocarbon systems, in which the intermolecular distances R are typically on the order of 3 to 4 Å.[25,32] In contrast the

separation between parallel macrocycles in hydrated Chl *a* aggregates is ~6 Å.[33,34] We thus expect electron exchange interactions, the strength of which varies as R^{-1}, to be significantly weaker in hydrated Chl *a* aggregates than in aggregate systems composed of aromatic hydrocarbons such as napthalene,[25] anthracene,[25,32] and pyrene.[35]

The electrostatic interactions between transition charge distributions responsible for the resonance coupling leading to formation of exciton states, approximated by transition dipole–dipole interactions,[36] are spin allowed in the triplet state in second-order perturbation theory. The triplet eigenstate $|T_1\rangle$ of a hydrated Chl *a* aggregate contains an admixture of the first excited singlet state,

$$|T_1\rangle = |\phi_{T_1}\rangle + \lambda\,|\sigma_{S_1}\rangle, \tag{27}$$

where $|\sigma_{S_1}\rangle$ and $|\phi_{T_1}\rangle$ denote "pure" singlet and triplet states. The admixture parameter λ is obtained from spin-orbit coupling interaction $\hat{\Omega}$ in first-order perturbation theory, i.e.,

$$\lambda \propto \langle\phi_{S_1}|\hat{\Omega}|\phi_{T_1}\rangle/\Delta E \ll 1. \tag{28}$$

Thus the exciton interaction in $|T_1\rangle$, arising from spin-orbit interaction, being on the order of λ^2, is also expected to be small. The above considerations lead to the conclusion that the triplet decay rate for the aggregate is the same as that of the monomer and therefore independent of the aggregate size.

Temperature dependence studies on the triplet lifetimes were carried out on sample A and the results appear in Table II. No rise to a steady-state fluorescence was observed as in Fig. 9 for either Chl *a*·H_2O or (Chl *a*·$2H_2O$)$_n$ above 180 K. Although the polymer triplet lifetime does not exhibit a temperature dependence between 159–80 K, the monomer exhibits a slight temperature dependence. The average of eight triplet lifetimes obtained at 77 K for the monomer with incident argon ion laser intensities (focused) in the range 32–100 mW/cm^2 was 1.1 ms with a standard deviation of 0.1 ms. The average of seven results for the polymer under the same conditions was 0.9 ms with a standard deviation of 0.2 ms. The measurements on (Chl *a*·H_2O)$_2$ were confined to 77 K because low temperatures are required to stabilize this aggregate *in vitro*.[20,21]

ODMR experiments[7] indicate that the triplet state lifetimes of Pheo *b* (2.2 ms) is less than that of Chl *b* (3.4 ms); the results in Table I reveal the same trend in Chl *a* (1.0 ± 0.2 ms) and Pheo *a* (0.6 ± 0.1 ms). The four N–Mg bonds in the chlorophyll species give rise to nonequivalent σ and π orbitals in two perpendicular directions within the porphyrin plane.[7] The more symmetric pheophytin molecule does not display such strong directional character. The spin sublevels associated with these in-plane molecular axes possess quite different kinetics in Chl *a*. This presumably results[7] in overall Chl *a* triplet state lifetimes perceptibly different from the corresponding values for Pheo *a*.

TABLE II. Temperature dependence of Chl *a* monomer and polymer triplet state lifetimes.

Species	Triplet Lifetime (ms)	T (K)
Chl *a*·H_2O	0.7 ± 0.1	155
	0.8 ± 0.1	140
	0.9 ± 0.2	117
	1.0 ± 0.2	77
(Chl *a*·$2H_2O$)$_n$	1.0 ± 0.1	159
	0.9 ± 0.1	148
	1.0 ± 0.1	125
	1.0 ± 0.1	114
	1.0 ± 0.1	102
	1.1 ± 0.2	91
	1.1 ± 0.2	80

There exist three independent spin levels in the Chl *a* T_1 state with unique $S_1 \rightarrow T_1$ and $T_1 \rightarrow S_0$ intersystem crossing rates. However, the highly temperature-dependent spin-lattice relaxation times are shorter than the triplet lifetimes at 77 K and therefore the triplet decay kinetics observed in this work would be well described by a single exponential. For this reason ODMR experiments are generally performed at 4 K. An experiment at 4 K on monomeric Chl *a* equivalent to our single-laser experiment at 77 K indicated a three-component exponential decay behavior.[18]

In the double-laser experiment the PMT is constantly exposed to sample fluorescence throughout the modulation cycle. This involved strong fluorescence due to simultaneous He–Ne and argon ion excitation and then weak fluorescence due only to the He–Ne laser during the sampling period. It was therefore necessary to demonstrate the ability of the complete detection system to rapidly and faithfully respond to the largely disparate fluorescent light levels incurred.[23] Although the fluorescence signal generated by the argon ion laser was strong, a PMT anode current of less than 3 μA was produced. This is well below the 1 mA limit for the PMT and detector saturation is not a concern. Experiments were designed to test the instrument response to fluorescence signals of well-known behavior and of the same magnitude as those generated by Chl *a* samples under actual experimental conditions. Results of these studies[23] indicated that the detection system accurately responds to sample fluorescence throughout the modulation cycle.

The formation of a long-lived triplet site in *in vitro* Chl *a*·H_2O aggregates (Table I and II) raises the possibility of participation of this state in photochemical reactions.[1,37–39] It has been suggested that a two-photon mechanism may play a significant role in the *in vivo* P680 photosynthetic light reaction.[1] The relationship between triplet-state formation and the subsequent singlet–triplet annihilation pathway of an *in vitro* Chl *a* system consisting primarily of (Chl *a*·$2H_2O$)$_n$ was identified in an earlier study.[23] The third term in Eq. (23) results from the excitation of T_1 to T_2. The presence of two-photon mechanisms leading to a shortening of the apparent triplet lifetime $\tau_T = \beta^{-1}$ thus provides an experimental criterion for establishing the four-level kinetic model.

Polycrystalline chlorophyll (Chl *a*·$2H_2O$)$_n$ is obtained[21,23] from monomeric Chl *a* as the predominant aggregate after several weeks of aging in a 10^{-4} M water-saturated nonpolar solution of Chl *a*, as in samples D and E. The effect of the aggregation process on the τ_T of (Chl *a*·$2H_2O$)$_n$ is shown in Fig. 10, in which the decay of fluorescence quenching, given by the second term in Eq. (21), is plotted as a function of time. It is evident that τ_T decreases to 0.6 ms on

sample aging as (Chl $a{\cdot}2H_2O)_n$ becomes the predominant aggregate (see inset, Fig. 10). The shortening of the triplet lifetime for (Chl $a{\cdot}2H_2O)_n$ is evidently a direct result of the singlet-triplet annihilation mechanism established earlier.[23] The four-level model for the fluorometic analysis of triplet decay kinetics presented in Sec. II is thus corroborated. These observations may account for the earlier finding[41] that τ_T for aggregated Chl a is $\sim$0.5 ms instead of 1 ms for the monomeric chlorophyll. From the above discussion it is evident that the Chl a triplet lifetime is not a simple function of the aggregate size n.

The observed variations in τ_T ranging from 0.5 to 2.0 ms were obtained[7,8,10–12,40,41] as a result of differences in the measurement method, solvation of the Chl a Mg atom by various nucleophiles, as well as any conceivable two-photon excitation processes. The data presented in Fig. 10 indicates that the aggregation interactions in (Chl $a{\cdot}2H_2O)_n$ appear in particular to favor singlet–triplet annihilation leading to the anomalous shortening of the triplet-state lifetimes of the chlorophyll.

ACKNOWLEDGMENT

The work reported in this paper was supported by a grant from the Basic Research Division of the Gas Research Institute.

[1]For a review, see F. K. Fong, in *Light Reaction Path of Photosynthesis*, edited by F. K. Fong, (Springer, New York, 1982), Vol. 35, Chap. 8.
[2]L. Galloway, D. R. Fruge, and F. K. Fong, Adv. Chem. Ser. **173**, 210 (1979).
[3]J. G. Brace, F. K. Fong, D. H. Karweik, V. J. Koester, A. Shepard, and N. Winograd, J. Am. Chem. Soc. **100**, 5203 (1978); F. K. Fong, J. S. Polles, L. Galloway, and D. R. Fruge, J. Am. Chem. Soc. **99**, 5802 (1977).
[4]F. K. Fong, M. Kusunoki, L. Galloway, T. G. Matthews, F. E. Lytle, A. J. Hoff, and F. A. Brinkman, J. Am. Chem. Soc. **104**, 2759 (1982).
[5]A. J. Alfano, F. E. Lytle, M. S. Showell, and F. K. Fong, J. Chem. Phys. **81**, 758 (1984).
[6]S. S. Dvornikov, V. N. Knyukshto, K. N. Solovyov, and M. P. Tsvirko, J. Lumin. **18/19**, 491 (1979).
[7]R. H. Clarke, Chap. 6 in Ref. 1.
[8]H. Linschitz and K. Sarkanen, J. Am. Chem. Soc. **80**, 4826 (1958).
[9]R. L. Livingston and P. J. McCartin, J. Phys. Chem. **67**, 2511 (1963).
[10]M. Hoshino, M. Imamura, K. Koike, K. Kikuchi, and H. Kokubun, Photochem. Photobiol. **38**, 255 (1983).
[11]C. A. Parker and T. A. Joyce, Photochem. Photobiol. **6**, 395 (1967).
[12]K. N. Solov'ev, S. S. Dvornikov, V. N. Knyukshto, and A. E. Turkova, J. Appl. Spectrosc. (USSR) **38**, 87 (1983).
[13]A. T. Gradyushko, S. S. Dvornikov, V. N. Knyukshto, and K. N. Solovev, Opt. Spectrosc. (USSR) **46**, 689 (1979).
[14]S. S. Dvornikov, V. N. Knyukshto, K. N. Solovev, and M. P. Tsvirko, Opt. Spectrosc. (USSR) **46**, 689 (1979).
[15]M. P. Tsvirko, K. N. Solovev, A. T. Gradyushko, and S. S. Kvornikov, Opt. Spectrosc, (USSR) **38**, 705 (1975).
[16]B. P. Straughen and S. Walker, *Spectroscopy* (Chapman and Hall, London, 1976), Vol. 3, pp. 161–198.
[17]N. Nakamizo and T. Matsueda, J. Mol. Spectrosc. **27**, 450 (1968).
[18]R. Avarmaa, Chem. Phys. Lett. **46**, 279 (1977).
[19]H. H. Strain, M. R. Thomas, and J. J. Katz, Biochim. Biophys. Acta **75**, 306 (1963).
[20]M. Hoshino, K. Ikehara, M. Imamura, H. Seki, and Y. Hama, Photochem. Photobiol. **34**, 75 (1981).
[21]F. K. Fong and V. J. Koester, Biochim. Biophys. Acta **423**, 52 (1976).
[22]J. H. C. Smith and A. Benitez, in *Modern Methods of Plant Analysis*, edited by K. Paech and M. V. Tracey (Springer, Berlin, 1955).
[23]A. J. Alfano and F. K. Fong, J. Am. Chem. Soc. **104**, 2767 (1982).
[24]H. J. Den Blanken and A. J. Hoff, Biochim. Biophys. Acta **724**, 52 (1983).
[25]E. J. P. Malar and A. K. Chandra, Theor. Chim. Acta **55**, 153 (1980).
[26]T. Kobayashi and N. Hirota, Bull. Chem. Soc. Jpn. **50**, 1743 (1977).
[27]T. Ohno and S. Kato, Chem. Lett. **3**, 263 (1976).
[28]D. Webster, J. F. Baugher, B. T. Lim, and E. C. Lim, Chem. Phys. Lett. **77**, 294 (1981).
[29]F. K. Fong, Appl. Phys. **6**, 151 (1975).
[30]D. P. Craig and S. H. Walmsley, *Excitons in Molecular Crystals* (Benjamin, New York, 1968).
[31]F. K. Fong and W. A. Wassman, J. Am. Chem. Soc. **99**, 2375 (1977).
[32]H.-H. Perkampus and H. Stichtenoth, Z. Phys. Chem. **76**, 18 (1971).
[33]R. J. Abraham and K. M. Smith, J. Am. Chem. Soc. **105**, 5734 (1983).
[34]V. J. Koester and F. K. Fong, J. Phys. Chem. **80**, 2310 (1976).
[35]J. B. Birks and A. A. Kazzaz, Proc. R. Soc. London Ser. A **304**, 291 (1968).
[36]A. J. Hoff, in Chap. 4 of Ref. 1.
[37]F. K. Fong, Proc. Natl. Acad. Sci. USA **71**, 3692 (1974).
[38]G. R. Seely, in *Current Topics in Bioenergetics*, edited by L. P. Vernon and D. R. Sanadi (Academic, New York, 1978), Vol. 7, pp. 29–73.
[39]J. R. Harbour and G. Tollin, Photochem. Photobiol. **19**, 163 (1974).
[40]H. Levanon and J. R. Norris, in Chap. 5 of Ref. 1.
[41]P. Mathis and P. Setif, Isr. J. Chem. **21**, 316 (1981).